© 2025 Journal of Pharmacy & Pharmacognosy Research, 13 (4), 1110-1119, 2025
ISSN 0719-4250
https://jppres.com

DOI: https://doi.org/10.56499/jppres24.2214_13.4.1110

Original Article

Radioiodinated bis-(α-mangostin)-cobalt (II) ([^{131}I]I-AM-Co): Radiolabelling, *in vitro* and *in vivo* evaluation for breast cancer radiopharmaceutical

[Bis-(α-mangostina)-cobalto (II) radioyodado ([^{131}I]I-AM-Co): Radiomarcaje, evaluación *in vitro* e *in vivo* para radiofármacos contra el cáncer de mama]

Richa Mardianingrum[1*], Susanti Susanti[1], Muchtaridi Muchtaridi[2,3], Ruswanto Ruswanto[4], Ine Suharyani[5], Amira M. Gazzali[6], Isti Daruwati[2,7], Ahsanal Fikri[7], Asep Rizaludin[6], Alfian M. Forentin[7], Wening Lestari[7], Veronika Y. Susilo[7], Dwi Ramadhani[7], Boky J. Tuasikal[8]

[1]Pharmacy Program, Faculty of Health Science, Universitas Perjuangan, Tasikmalaya 46115, West Java, Indonesia.
[2]Research Collaboration Center for Theranostic Radiopharmaceuticals, Jl Ir. Soekarno KM 21, Jatinangor 45363, Indonesia.
[3]Department of Pharmaceutical Analysis and Medicinal Chemistry Faculty of Pharmacy, Padjadjaran University, Jatinangor, Sumedang 45363, West Java, Indonesia.
[4]Pharmacy Program, Universitas Bakti Tunas Husada, Tasikmalaya 46115, West Java, Indonesia.
[5]Faculty of Pharmacy, Universitas Muhammadiyah Ahmad Dahlan, Cirebon 45153, West Java, Indonesia.
[6]School of Pharmaceutical Sciences, Universiti Sains Malaysia, Penang, Malaysia.
[7]Research Center for Radioisotope, Radiopharmaceutical, and Biodosimetry Technology, Research Organization for Nuclear Energy, National Research and Innovation Agency (BRIN), Jl Puspiptek - Kota Tangerang Selatan, Indonesia.
[8]Radiation Process Technology Research Center, Jl Puspiptek - Kota Tangerang Selatan, Indonesia.
*E-mail: richamardianingrum@unper.ac.id

Abstract

Context: The development of radiopharmaceuticals derived from natural compounds has been extensively studied, particularly for cancer treatment. α-Mangostin is a molecule claimed to be toxic to cancer cells, and its derivative, an organometallic compound, has been synthesized successfully, namely bis-(α-mangostin)-cobalt(II) or AM-Co. The AM-Co structure shows promise as a radiopharmaceutical candidate, especially when labelled with radioactive iodine.

Aims: To optimise the radiolabelling conditions of AM-Co with iodine-131 and assess its internalization profile in breast cancer cell lines, as well as biodistribution and pharmacokinetic profile using *in vivo* approaches.

Methods: The radiolabelling of [^{131}I]I-AM-Co was carried out by electrophilic aromatic substitution, with CATas the oxidising agent at low temperatures for synthesis. Internalization studies of [^{131}I]I-AM-Co were conducted in MCF-7 cell lines. Additionally, the biodistribution and pharmacokinetic profiles were assessed by administering 0.37–1.11 MBq of [^{131}I]I-AM-Co (i.v. route) in normal mice and rats.

Results: The [^{131}I]I-AM-Co was successfully synthesized with radiopharmaceutical purity of 99.12 ± 0.18% and internalized into MCF-7 cell lines greater than 46% after one hour of incubation. In addition, [^{131}I]I-AM-Co demonstrates 11 times slower diffusion from blood into organs compared with iodine -131, with $t_{½}$ α was 0.33 ± 0.17 hour. Interestingly, based on AUC data, it reveals that systemic exposure of [^{131}I]I-AM-Co exhibits increasing five times than iodine-131. However, the highest accumulation of [^{131}I]I-AM-Co was still found in the thyroid gland.

Conclusions: The [^{131}I]I-AM-Co can be synthesized, achieving a radiochemical purity of over 90%. In addition, the [^{131}I]I-AM-Co compound greatly enhances cellular uptake and plasma concentration compared to iodine-131, which exhibits rapid clearance.

Keywords: breast cancer; cobalt; mangostin; radiopharmaceutical.

Resumen

Contexto: Los radiofármacos derivados de compuestos naturales ha sido ampliamente estudiado, en particular para el tratamiento del cáncer. La α-mangostina, una molécula tóxica para las células cancerosas, y su derivado, un compuesto organometálico, se ha sintetizado con éxito, concretamente el bis-(α-mangostina)-cobalto(II) o AM-Co. AM-Co es un candidato a radiofármaco prometedor, especialmente cuando se marca con yodo radiactivo.

Objetivos: Optimizar las condiciones de radiomarcaje del AM-Co con yodo-131 y evaluar su perfil de internalización en líneas celulares de cáncer de mama, así como su biodistribución y perfil farmacocinético mediante métodos *in vivo*.

Métodos: El radiomarcaje del [^{131}I]I-AM-Co se llevó a cabo mediante sustitución aromática electrofílica, con CAT como agente oxidante a bajas temperaturas para la síntesis. Se realizaron estudios de internalización de [^{131}I]I-AM-Co en líneas celulares MCF-7. Además, se evaluaron los perfiles de biodistribución y farmacocinética mediante la administración de 0,37–1,11 MBq de [^{131}I]I-AM-Co (vía intravenosa) en ratones y ratas normales.

Resultados: El [^{131}I]I-AM-Co se sintetizó con éxito con una pureza radiofarmacéutica del 99,12 ± 0,18% y se internalizó en líneas celulares MCF-7 en un porcentaje superior al 46% después de una hora de incubación. Además, el [^{131}I]I-AM-Co demuestra una difusión 11 veces más lenta desde la sangre a los órganos en comparación con el yodo-131, con un t½ α de 0,33 ± 0,17 horas. Curiosamente, según los datos de AUC, se revela que la exposición sistémica de [^{131}I]I-AM-Co aumenta cinco veces más que la del yodo-131. Sin embargo, la mayor acumulación de [^{131}I]I-AM-Co se encontró en la glándula tiroides.

Conclusiones: El [^{131}I]I-AM-Co se puede sintetizar, logrando una pureza radioquímica de más del 90%. Además, el compuesto [^{131}I]I-AM-Co mejora en gran medida la captación celular y la concentración plasmática en comparación con el yodo-131, que muestra una eliminación rápida.

Palabras Clave: cáncer de mama; cobalto; mangostina; radiofármaco.

ARTICLE INFO
Received: September 22, 2024.
Accepted: January 29, 2025.
Available Online: March 15, 2025.

AUTHOR INFO
ORCID:
0000-0003-2580-266X (RR)
0000-0002-2406-1356 (AF)
0000-0002-9926-5249 (VYS)
0000-0002-2327-363X (RM)
0000-0002-1649-9294 (IS)
0009-0009-4066-944X (AR)
0000-0003-3018-2485 (DR)
0000-0002-6288-2737 (SS)
0000-0003-4469-1969 (AMG)
0000-0003-2338-6172 (AMF)
0009-0003-0423-7590 (BJT)
0000-0002-6156-8025 (MM)
0000-0002-9389-8336 (ID)
0000-0002-0452-1984 (WL)

Abbreviations: AM-Co: bis-(α-mangostin)-cobalt(II); ROS: reactive oxygen species; CAT: chloramine-T; BC: breast cancer; ER: estrogen receptor; RCP: radiochemical purity; BRIN: National Research and Innovation Agency Republic of Indonesia; MAPK: mitogen-activated protein kinases; AGC: automatic gamma counter; AUC: area under the curve; CL: clearance; Vss: steady-state volume of distribution; MRT: mean residence time; %ID/g: percentage of injection dose per weight of animal organ sample in grams; TCA: trichloroacetic acid.

INTRODUCTION

Breast cancer (BC) remains the most prevalent malignancy among women, ranking first in both incidence and mortality in 2020, with 2.26 million new cases and a 15.5% mortality rate recorded globally (Bray et al., 2024). As cancer cases continue to rise, the International Agency for Research on Cancer projects that in 2024, there will be 19.9 million cases of cancer worldwide. The introduction of cisplatin in the early 1980s revolutionized cancer treatment, and this has not only resulted in the development of newer platinum-based drugs like carboplatin and oxaliplatin but also accelerated clinical trials of other platinum compounds and the exploration of anticancer properties of different transition metal complexes (Ruswanto et al., 2023; Zhang et al., 2022; Zhang and Sadler, 2017).

The previous study showed that α-mangostin could inhibit cell proliferation and induce apoptosis associated with HER2/PI3K/Akt and mitogen-activated protein kinases (MAPK) signalling pathway in human breast carcinoma T47D cells (Kritsanawong et al., 2016). Still, in another study, the absolute bioavailability of a-mangostin was low and exhibited minimal oral absorption (Li et al., 2011). Previously, we successfully synthesized bis-(α-mangostin)-cobalt(II) (AM-Co), which demonstrated selective antiproliferative activity against MCF-7 cell lines. It was classified as highly toxic (strong) against the cancer cells *in silico* and *in vitro* studies (Mardianingrum et al., 2024).

The development of radiopharmaceuticals based on natural compounds is currently being widely researched (Wongso, 2022). Among the technological approaches in theranostics is applying radiolabelled compounds with specific radioisotopes, especially iodine-131. Iodine can be labelled in flavonoid-based compounds because it can bind to the phenolic moiety with minimal changes to the compound's original structure (Daruwati et al., 2019; Nurhidayah et al., 2023). In addition, radiolabelling approaches are also used for biodistribution studies and biomedical imaging to track the biodistribution of natural compounds *in vivo* (Mahendra et al., 2018).

Several studies have also reported the successful synthesis of radioiodine-labelled flavonoids and their applications for biodistribution and imaging studies. ^{125}I-labeled rutin was administered both orally and intravenous. Injected ^{125}I-labeled rutin was accumulated in the small intestine within 1 hour. This result underlies the use of iodine in radiolabelling other flavonoids or natural compounds to investigate their biodistribution (Silberstein et al., 2012).

In particular, AM-Co compounds have been shown to have activity against MCF-7 and T47D cell lines, thereby inhibiting cell growth (Mardianingrum et al., 2024). Also in radiopharmaceutical fields, these findings encourage further studies. Based on the AM-Co chemical structure, iodine-131 labeling is definitely possible. Furthermore, the activity biology of radiolabelled AM-Co for theragnostic application needs to be further evaluated through *in vitro* and *in vivo* studies.

MATERIAL AND METHODS

Material

Radioisotope of iodine-131, as the main material, was irradiated in multipurpose nuclear reactor G.A. Siwabessy, National Research and Innovation Agency Republic of Indonesia (BRIN). All chemical reagents were purchased from Sigma Aldrich, including chloramine-T (CAT), sodium metabisulfite, ethanol, dimethyl sulfoxide (DMSO), sodium hydroxide, and pH paper. Whatman No.1 paper (GE Health), injection spuit G27 (Onemed), water for injection (IPHA), 24-well plate (TPP). Cell culture growth mediums were purchased from Gibco, including RPMI-1640, fetal bovine serum, penicillin-streptomycin, amphotericin B, and Hanks' Balanced Salt Solution (HBSS). The instruments used are Automatic Gamma Counter (Perkin Elmer), RadioTLC Scanner (Comecer), dose calibrator (Caprac-T), analytical balance (Metler Toledo), cold storage, and digital shaking dry bath (Thermo Scientific).

Animal

Male Sprague-Dawley rats (200-300 g, age range 8-12 weeks) and male BALB/c mice were purchased from Biomedical Technology Indonesia (BMTI). All animal research protocols in this experiment were approved by the Animal Care Ethics Committee – BRIN with approval number 28062024000002 and the Nuclear Energy Ethics Committee – BRIN with approval number 15072024000021.

[^{131}I]I-AM-Co radiolabelling optimization and radiochemical purity determination

The electrophilic aromatic substitution method was used to label AM-Co by oxidising iodine-131 with CAT (Daruwati et al., 2017; Durante et al., 2019;

Muftuler et al., 2008). Optimization was achieved by adjusting the amount of ligands (AM-Co) and CAT, as well as varying incubation time and temperature. 100-300 µg of AM-Co in DMSO was added with 25-125 µg of CAT in phosphate buffer, pH 8. The mixture was then homogeneously, followed by adding 2-4 µL of iodine-131 (radioactivity 11.1-18.5 MBq). Thereafter, the solution was incubated at 2-4 and 25°C for 15-30 minutes with constant agitation. Following the incubation, the reaction was stopped by adding 1 µL of 50 mg/mL sodium metabisulfite in phosphate buffer, pH 7.5-8. The radiolabelling compound was characterised by assessing the RCP using paper chromatography. Two microlitres of the radiolabelled compound were applied to Whatman Paper No. 1 and eluted with 0.01 M phosphate buffer, pH 8.0, under electrophoresis conditions for one hour at 250 volts. After the paper dried, radioactivity was measured using a Radio TLC-Scanner. The radiolabelled of [^{131}I]I-AM-Co the required radiochemical purity standards when its percentage was greater than 95%. Furthermore, to validate the radiolabelling result, the [^{131}I]I-AM-Co RCP was measured by radio-HPLC (Daruwati et al., 2019)

Stability of [^{131}I]I-AM-Co

The stability of [^{131}I]I-AM-Co was evaluated by determining the RCP of the radiolabelled compound stored at 4°C (refrigerator) and -20°C (freezer).

Physicochemical characterization

The [^{131}I]I-AM-Co was characterised by lipophilicity and plasma binding protein tests. The lipophilicity of [^{131}I]I-AM-Co was assessed by determining its distribution coefficient between n-octanol and an aqueous phase. The log P value was calculated as the logarithm of the ratio of the fractions in these phases. Blood plasma and a radiolabelled compound [^{131}I]I-AM-Co were mixed in test tubes to assess plasma protein binding. After incubation, trichloroacetic acid (TCA) was added to separate bound and unbound fractions. Centrifugation was performed to isolate the protein-bound fraction (precipitate). The precipitate was washed, and the radioactivity in both the precipitate and the supernatant was measured to determine the percentage of the radiolabelled compound bound to plasma proteins.

Cellular uptake of [^{131}I]I-AM-Co against MCF-7 cells

The internalization profile was evaluated using MCF-7 cell lines at various periods of time. Cultured cells were incubated in RPMI supplemented with 10% fetal bovine serum, 100 units/mL penicillin, 100 µg/mL streptomycin, and 2.5 µg/mL amphotericin B in 24-well plates. The cells were collected individually using a micropipette and then rinsed with 500 µL of HBSS sample solution containing 0.037 MBq/mL of [^{131}I]I-AM-Co. The same radioactivity of Iodine-131, as a control, was added to the triplicate wells. Subsequently, treated cells were incubated at 37°C for 10, 30, and 60 minutes. After incubation, the samples were removed and washed twice using cold PBS. Finally, the cells were lysed by adding 60 µL of 0.2 N NaOH. The radioactivity of each cell lysate was measured using an automatic gamma counter. The cellular uptake of the samples was analysed by comparing the results to the standards (Wongso et al., 2023).

Pharmacokinetic study

The pharmacokinetic profile of [^{131}I]I-AM-Co was evaluated *in vivo* using three rats per group. 150 µL of 0.37-1.11 MBq [^{131}I]I-AM-Co was administered intravenously by the tail vein. Blood samples were collected at specified time points post-injection (5 mins, 0.5, 1, 3, 5, 24, 48, 72, and 96 h) from the tail of each rat (Mahendra et al., 2018). Furthermore, control groups were administered with iodine-131 at equivalent radioactivity of [^{131}I]I-AM-Co. The samples were then weighed, and radioactivity was quantified using an automatic gamma counter. The results were expressed as the percentage of injected dose per gram of blood (% ID/g) (Tishchenko et al., 2017).

Biodistribution study

The biodistribution of [^{131}I]I-AM-Co in the living organism was investigated in mice at various time intervals: 0.5, 1, 2, 3, 24, 48, 72, and 96 h. One hundred microliters of 0.37-1.11 MBq [^{131}I]I-AM-Co were delivered to three mice in each group. Upon reaching each designated time point, the mice were euthanised via i.p. administration of ketamine/xylazine. All organs utilised for these investigations were collected, including bone, large intestine, liver, spleen, kidney, lung, heart, stomach, thyroid, skin, muscle, and blood. The samples were weighed, and the radioactivity of the organs was quantified using an automatic gamma counter. The percentage of radioactive accumulation in each organ was then calculated. This calculation was subsequently compared to iodine-131 administered as a control. The organ uptakes were calculated as the percent of the area under the curve of the related photo-peak per g of an organ (% ID/g) (Muftuler et al., 2008; Wongso et al., 2022).

Statistical analysis

In this study, all data were obtained from three replication experiments. Statistical differences in biodistribution among organs were determined using

two-way ANOVA ($p<0.01$). The cellular uptake and pharmacokinetic profiles of iodine-131 and [^{131}I]I-AM-Co were statistically compared using an independent t-test ($p<0.01$). Radiolabelling results were evaluated statistically using one-way ANOVA or independent *t*-test ($p<0.01$). All graphs were produced utilising GraphPad Prism version 10.3.1.

RESULTS AND DISCUSSION

α-Mangostin, a major compound from the pericarp of the mangosteen fruit (*Garcinia mangostana* L.), has attracted considerable interest for its potential as a natural anticancer (Majdalawieh et al., 2024). α-Mangostin inhibits cancer cell growth through numerous mechanisms, including the induction of pro-apoptotic effects via the estrogen receptor (ER) (Won et al., 2014), ROS-mediated endoplasmic reticulum stress through the WNT pathway (Yang et al., 2021), and activates ASK1/p38 signaling pathway (Lee et al., 2017). Considering its potential anti-cancer effects, α-mangostin presents various difficulties restricting its clinical implementation (Majdalawieh et al., 2024). Previous research revealed a successful synthesis of a metal complex of α-mangostin, that is, α-mangostin complexed with cobalt (AM-Co), which has shown enhanced efficacy as an anticancer agent against breast and cervical cancer (Mardianingrum et al., 2024). The initial characterization of the AM-Co compound was conducted using the HPLC method with a C-18 column. The analysis utilized a 90% MeCN mixture under isocratic conditions, with a flow rate of 1 mL/min and a detection wavelength of 254 nm. As shown in Fig. 1A, the single peak corresponding to AM-Co was observed at a retention time of 3.28 minutes, with an area under the curve (AUC) value of 16,093.91.

Radiopharmaceuticals are widely used for cancer treatment, including imaging and therapy. Natural compound-based radiopharmaceuticals have been studied and developed because of their promising potential and suitability of chemical structure to be labeled with radioisotopes, especially iodine-131 (Daruwati et al., 2023; Wongso, 2022). Based on previous studies, the biological potency and structural compatibility of AM-Co rendered it a viable ligand for a radiopharmaceutical candidate. The electrophilic radioiodination of AM-Co with iodine-131 was conducted using CAT as a strong oxidizing agent. In this process, iodine was introduced as NaI, and an oxidation step was carried out to convert NaI to its highly reactive form, I^+ by CAT (Durante et al., 2019). The final product of [^{131}I]I-AM-Co was characterized using the radioelectrophoresis method to measure RCP. According to RCP characterization, the formation of [^{131}I]I-AM-Co exceeded 90%. The radiochromatogram in Fig. 1 displays the differences in retention factors between [^{131}I]I-AM-Co (Fig. 1C) and iodine-131 (Fig. 1B), with iodine-131 migrating from the application point to the anode terminal of the electrophoresis chamber because iodine-131 more negative than [^{131}I]I-AM-Co (Daruwati et al., 2019).

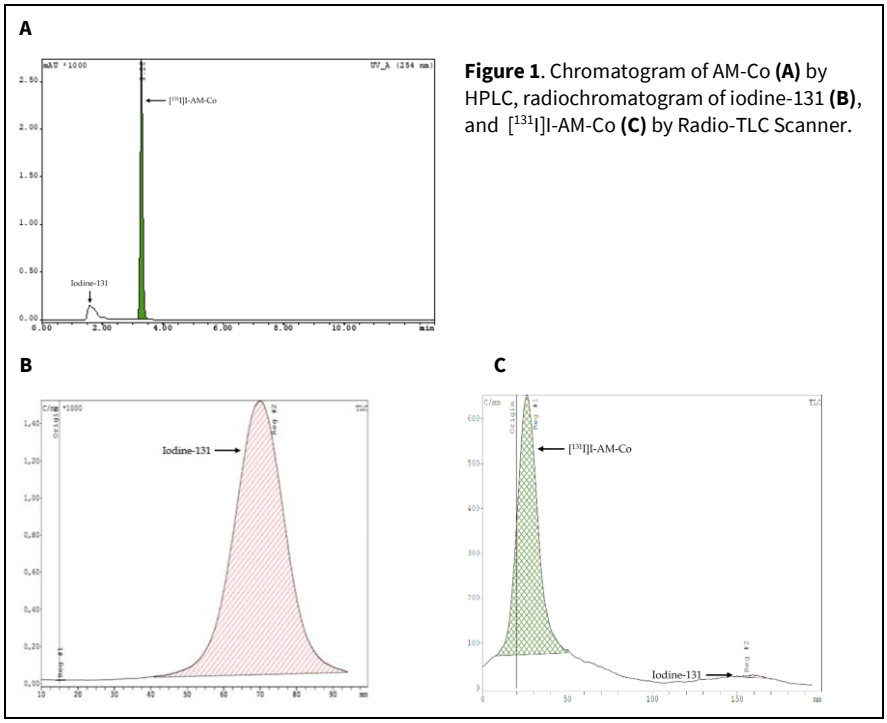

Figure 1. Chromatogram of AM-Co **(A)** by HPLC, radiochromatogram of iodine-131 **(B)**, and [^{131}I]I-AM-Co **(C)** by Radio-TLC Scanner.

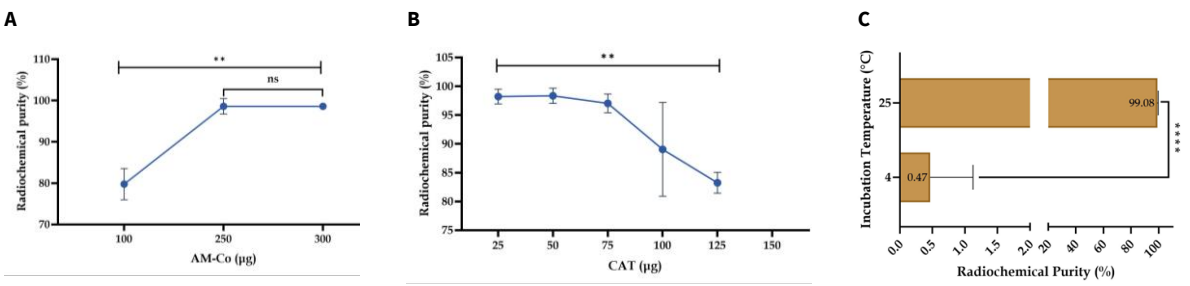

Figure 2. Optimisation radiolabelling of [^{131}I]I-AM-Co.

(A) Effect of ligand; **(B)** Effect of CAT; and **(C)** Effect of incubation temperature. Data are expressed as mean ± SD (n = 3), **p<0.05 statistical analysis using independent t-test and one-way ANOVA, CI: 99%.

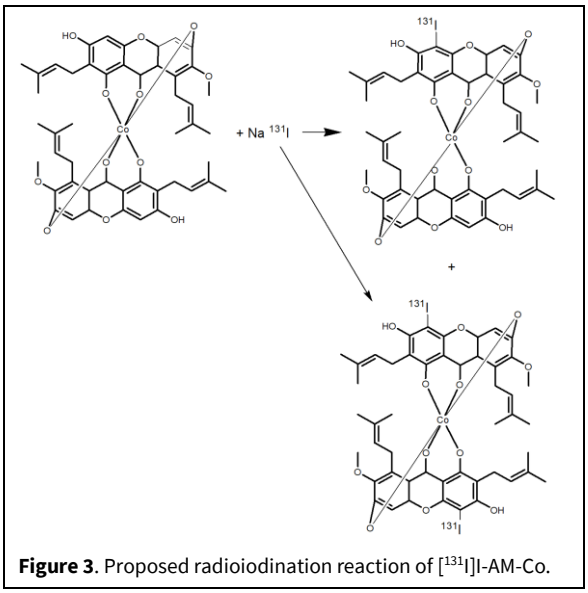

Figure 3. Proposed radioiodination reaction of [^{131}I]I-AM-Co.

The iodine-131 compound, a clear solution, exhibits a migration distance of 0.8-0.9 cm from the application point towards the anode with an RCP of 99.62 ± 0.52% (n = 5). In contrast, the [^{131}I]I-AM-Co compound displays a yellow-clear appearance, an RF value of 0.0-0.2, and an RCP of 99.12 ± 0.18% (n = 3). Optimal results were achieved by varying the quantities of ligands and CAT and adjusting the incubation and reaction times. The amount of ligands significantly influences the outcome; too many ligands can lead to an excess of unbound ligands, which may interfere with receptor binding. Therefore, the optimal quantity was determined to be 250 µg of AM-Co (see Fig. 2A), combined with a minimal amount of CAT at 25 µg (see Fig. 2B). The compound [^{131}I]I-AM-Co was produced with a high RCP at a low reaction temperature of 2-4°C over a 30-minute period (see Fig. 2C).

Electrophilic substitution is the reaction that facilitates the formation of radioiodine-labeled compounds. An iodine atom substitutes a hydrogen atom in a stable position on the carbon backbone of AM-Co, particularly between the two ether groups in the structure (Fig. 3). The carbon atoms in this region are more prone to connect with the electrophilic [^{131}I] due to their electron-rich environment, which can stabilise the new iodine bond. Moreover, CAT has been widely used as an oxidizing agent for radioiodine in the electrophilic labeling of phenolic compounds (Baldwin and Lin, 1981; Sriyani et al., 2019). In this study, we used various amounts of CAT to induce the oxidizing of iodine-131.

The stability of [^{131}I]I-AM-Co was conducted over 9 days. From days 2 to 9, the compounds stored at -20°C exhibited higher RCP than those stored at 2-4°C. Notably, both groups experienced a similar decrease in RCP on day 8 (see Fig. 4A). Additionally, tests were performed on PBS and plasma solutions over 24 hours. In the PBS solution (Fig. 4B), the radiochemical purity of the marked compounds began to decline after the 3rd hour. In contrast, the purity in the plasma solution (Fig. 4C) decreased starting at the 2nd hour. By the end of the 24 hours, the PBS and plasma solutions significantly decreased in RCP, below 80%. Overall, the radiolabelled [^{131}I]I-AM-Co shows good stability when stored at cold temperatures and in the freezer. However, its stability significantly decreases

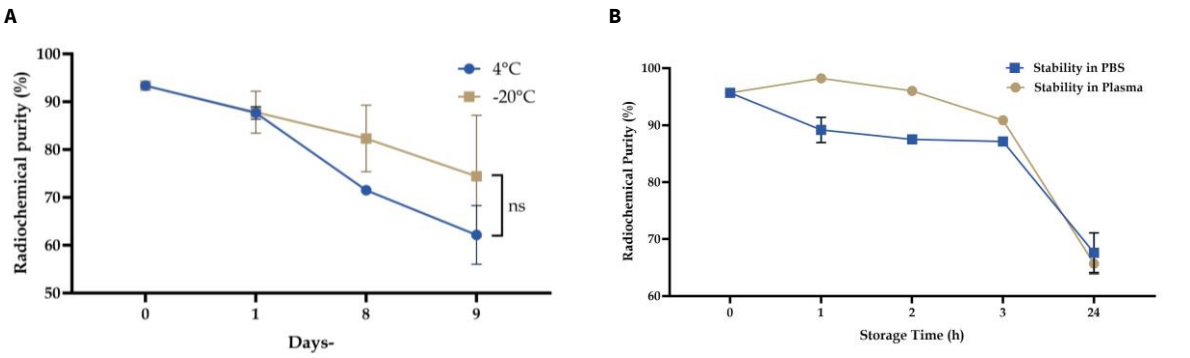

Figure 4. Stability Radiolabelling of [^{131}I]I-AM-Co.

(A) Storage temperature; **(B)** PBS and **(C)** Plasma.

Data are expressed as mean ± SD (n = 3), ns: p>0.05 statistical analysis using independent t-test and one-way ANOVA, CI: 99%.

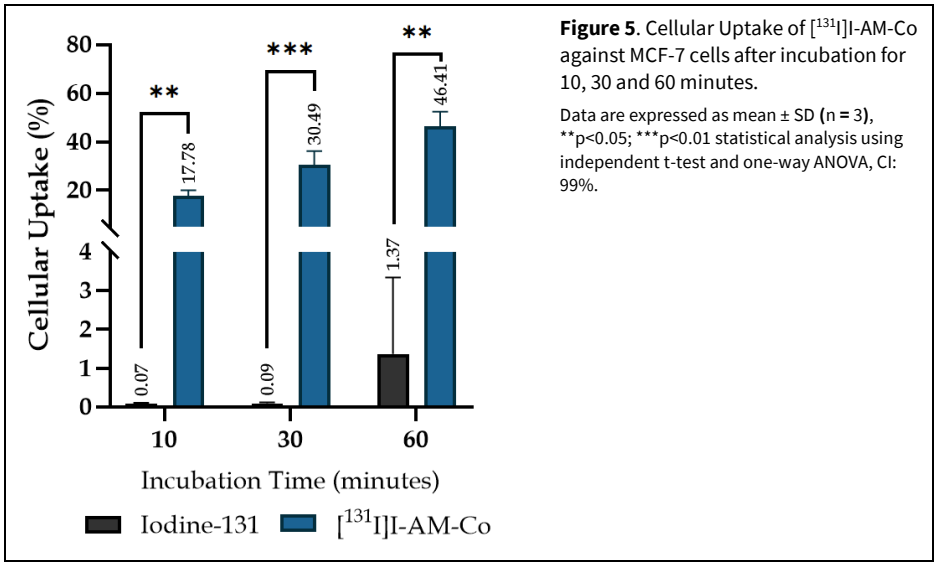

Figure 5. Cellular Uptake of [^{131}I]I-AM-Co against MCF-7 cells after incubation for 10, 30 and 60 minutes.

Data are expressed as mean ± SD **(n = 3)**, **p<0.05; ***p<0.01 statistical analysis using independent t-test and one-way ANOVA, CI: 99%.

when stored in PBS solution with a pH of 7.4 or in plasma at 37°C over 24 hours. Furthermore, the physicochemical characterization results indicated that [^{131}I]I-AM-Co revealed lipophilic characteristics, with a log-P value of 0.789 ± 0.119, and approximately 93.20 ± 0.488% of [^{131}I]I-AM-Co was found to be bound in plasma proteins.

An *in vitro* study of [^{131}I]I-AM-Co was performed to assess internalization in MCF-7 cell lines. The results showed that the cellular uptake of [^{131}I]I-AM-Co was significantly distinct from that of iodine-131. The uptake profile revealed a progressive increase over the incubation period, with the highest uptake reaching 46% after one hour, as depicted in Fig. 5. MCF-7 cells are human breast cancer cells that mostly express estrogen receptor (ER)-α and also exhibit slight expression of ER-β (Dagher et al., 2012; Vantangoli et al., 2015). Previous studies reported that AM-Co exhibits a stronger binding affinity for ER-α compared to α-mangostin and cisplatin (Mardianingrum et al., 2024). These results suggest that AM-Co can facilitate the accumulation of iodine-131 inside MCF-7 cell lines.

The blood clearance profile evaluation for [^{131}I]I-AM-Co, as shown in Table 1, provides information on its pharmacokinetics over time, including the half-life ($t_{1/2}$), clearance rate, and overall bioavailability following administration to the animal model. The pharmacokinetic analysis demonstrates that [^{131}I]I-AM-Co significantly affects key pharmacokinetic parameters, including the elimination half-life ($t_{½}$ β), area under the curve (AUC), clearance (CL), and steady-state volume of distribution (Vss). Both [^{131}I]I-AM-Co and Na[^{131}I] follow a two-compartment pharmacokinetic model, which encompasses both the initial distribution phase and the terminal elimination phase, as illustrated in Fig. 6.

Half-life ($t_{½}$ α) of [^{131}I]I-AM-Co showed a rapid change in distribution from the blood to the organ with rapid perfusion at 0.33 hours or the equivalent of 19.8 minutes. This is slower than iodine-131 as the

Table 1. Pharmacokinetic data of [^{131}I]I-AM-Co and iodine-131 in rats.

Parameter	Unit	[^{131}I]I-AM-Co	Iodine-131
$t_{½}$ α*	h	0.33 ± 0.17	0.03 ± 0.01
$t_{½}$ β**	h	6.37 ± 0.10	7.44 ± 0.02
AUC $_{(0-\infty)}$**	%ID/mL	39.73 ± 4.96	7.82 ± 0.06
CL**	mL/g/h	2.90 ± 0.27	12.80 ± 0.49
Vss**	mL/g	27.95 ± 1.52	137.93 ± 5.69
MRT $_{(0-\infty)}$*	h	9.67 ± 0.39	10.77 ± 0.03

Data represent mean ± SD (n = 3). *p>0.05 indicates not significantly different with unpaired t-test. **p<0.05 indicates a significant difference with unpaired t-test.

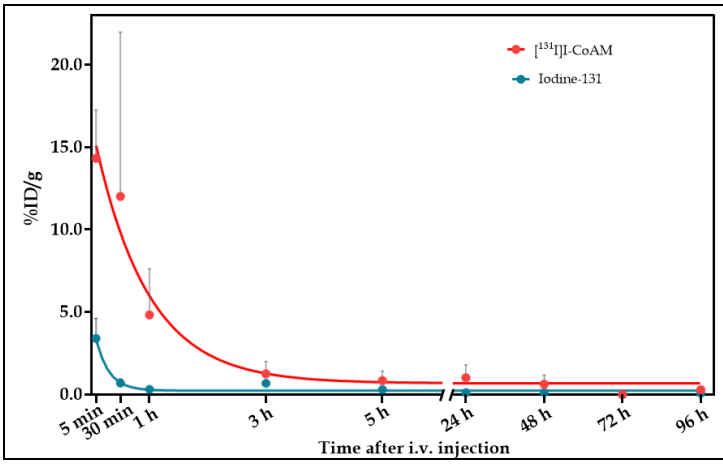

Figure 6. Blood clearance profiles of [^{131}I]I-AM-Co and iodine-131 in rats. Data were determined by AGC, presented as %ID/g ± SD. Data represent mean clearance of samples ± SD (n = 3).

radioactive control, which has a very fast $t_{½}$ α at 1.8 min. This suggests that the distribution of more non-polar radiolabel compounds affects their distribution in the blood. Significant differences also in $t_{½}$ β and AUC of [^{131}I]I-AM-Co suggest that the compound has a shorter elimination half-life and greater systemic exposure than Na[^{131}I]. The marked reduction in CL and Vss for [^{131}I]I-AM-Co in comparison to Na[^{131}I] indicates slower clearance and a limited distribution at steady-state.

Despite the differences in elimination profiles, the mean residence time (MRT) for both [^{131}I]I-AM-Co and Na[^{131}I] is similar, with values of 9.67 hours and 10.77 hours, respectively, implying that both compounds remain in the body for comparable durations (Table 2). The pharmacokinetic curves reflect these dynamics, with [^{131}I]I-AM-Co exhibiting a significantly higher and faster initial distribution, while Na[^{131}I] shows a slower and more gradual distribution over the same period.

The biodistribution results of [^{131}I]I-AM-Co in rat tissues (%ID/g) are presented in Table 2. Effective retention of the compound was demonstrated in the skin, muscle, blood, large (L) intestines, kidney, spleen, liver, heart, lung, thyroid, stomach, and bone tissues. The biodistribution profile of [^{131}I]I-AM-Co and iodine-131 after one hour of injection were different in each organ, Fig. 7A. Iodine-131 accumulated in thyroid glands. This phenomenon is in accordance with its natural ability (Iglesias et al., 2017). This can be seen at the 24 and 48 hours when the [^{131}I]I-AM-Co entering the thyroid gland reached 67.3143 and 63.7942%, respectively. Meanwhile, at 96 hours, elimination began to occur, marked by a decrease in ID to 1.625%.

Distribution in the stomach, intestines, and blood looks high in the first half hour but is still smaller than in the thyroid. The highest %ID/g of [^{131}I]I-AM-Co in important organs for distribution, metabolism, and excretion was observed 30 minutes post-i.v. administration, followed by a progressive decline over time (Fig. 7B). In addition, specific amounts of [^{131}I]I-AM-Co were found in several organs, such as the liver (0.138 %ID/g), lungs (0.284%ID/g), and kidneys (0.1378 %ID/g) at the same time, 24 hours. These results align with previous studies showing that the consumed routine is absorbed in the L intestine (Choi et al., 2016).

These findings suggest that the development of radiopharmaceuticals using natural substances as radioisotope carriers may be an appropriate approach. Nonetheless, further study is required for a

Table 2. Biodistribution profile of [^{131}I]I-AM-Co compound in normal mice.

Organ	%ID/g							
	30 min	1 h	2 h	3 h	24 h	48 h	72 h	96 h
Skin	0.893 ± 0.34	1.339 ± 0.56	0.274 ± 0.17	0.700 ± 0.54	0.139 ± 0.11	0.209 ± 0.26	0.088 ± 0.10	0.018 ± 0.08
Muscle	0.425 ± 0.11	0.371 ± 0.03	0.178 ± 0.12	0.195 ± 0.13	0.074 ± 0.03	0.212 ± 0.28	0.062 ± 0.14	0.117 ± 0.21
Bone	0.872 ± 0.22	0.673 ± 0.10	0.475 ± 0.20	0.481 ± 0.27	0.060 ± 0.00	0.623 ± 0.90	0.139 ± 0.50	0.081 ± 0.14
Blood	3.580 ± 1.04	2.764 ± 0.65	1.202 ± 0.48	1.536 ± 1.43	0.207 ± 0.07	0.748 ± 1.04	0.072 ± 0.05	0.722 ± 1.24
Intestine	2.236 ± 1.36	1.506 ± 0.61	1.493 ± 1.61	0.851 ± 0.87	0.138 ± 0.03	0.134 ± 0.17	0.061 ± 0.09	0.038 ± 0.06
Liver	1.261 ± 0.29	0.877 ± 0.34	0.587 ± 0.11	0.445 ± 0.33	0.138 ± 0.02	0.148 ± 0.04	0.077 ± 0.06	0.081 ± 0.11
Spleen	2.153 ± 1.11	1.110 ± 0.60	0.532 ± 0.13	0.359 ± 0.10	0.109 ± 0.04	0.193 ± 0.23	0.064 ± 0.21	0.075 ± 0.13
Kidney	1.760 ± 1.52	1.524 ± 0.37	0.446 ± 0.22	0.423 ± 0.18	0.138 ± 0.04	0.224 ± 0.16	0.127 ± 0.16	0.169 ± 0.26
Heart	0.885 ± 0.16	1.019 ± 0.41	0.399 ± 0.25	0.394 ± 0.19	0.101 ±0.02	0.194 ± 0.22	0.145 ± 0.22	0.107 ± 0.19
Lung	1.433 ± 0.39	1.196 ± 0.20	0.668 ± 0.24	0.719 ± 0.40	0.281 ± 0.10	0.214 ± 0.24	0.227 ± 0.54	0.111 ± 0.19
Thyroid	10.220 ± 4.88	12.965 ± 1.12	26.748 ± 21.23	9.106 ± 0.61	67.314 ± 33.42	63.794 ± 45.19	N/A	1.625 ± 2.82
Stomach	5.796 ± 2.11	3.600 ± 1.76	5.414 ± 4.33	2.970 ± 3.03	0.720 ± 0.48	0.156 ± 0.21	0.060 ± 0.08	0.031 ± 0.05

[^{131}I]I-AM-Co is bis-(α-mangostin)-cobalt(II) labelled with iodine-131 . The data are expressed as the means ± SD of three independent experiments.

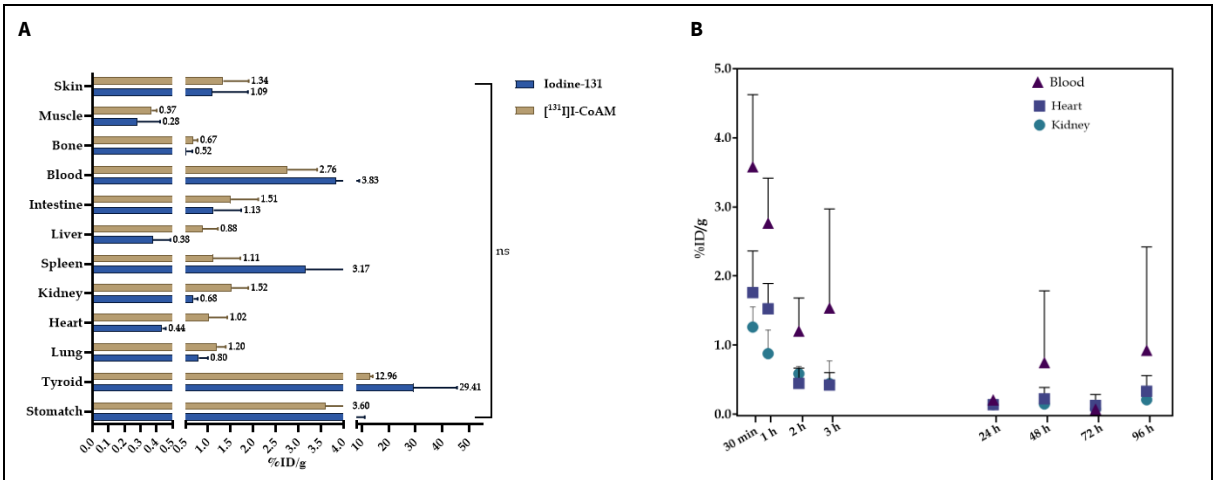

Figure 7. Comparison biodistribution of [^{131}I]I-AM-Co against iodine-131 after one-hour post i.v. injection **(A)**. Distribution profile of [^{131}I]I-AM-Co in important organs in pharmacology studies **(B)**.

Data are presented as %ID/g ± SD and analised by independent t-test, p<0.05.

comprehensive understanding. It is essential to investigate the death mechanism of [^{131}I]I-AM-Co at the DNA level and compare it with normal cell lines. Moreover, the anticancer activity in animal models of cancer must be assessed to determine the effectiveness of [^{131}I]I-AM-Co as an anticancer agent in nuclear medicine.

CONCLUSION

The radiolabelled [^{131}I]I-AM-Co was successfully produced with a high purity of 99.12 ± 0.18%. The internalization of [^{131}I]I-AM-Co was significantly distinct from that of iodine-131, with the highest uptake reaching 46% after one hour. In addition, [^{131}I]I-AM-Co exhibits a fast pharmacokinetic profile characterized by rapid distribution and clearance. Iodine-131, on the other hand, shows a more sustained retention, with a slower decline in concentration over time.

CONFLICT OF INTEREST

The authors declare no conflicts of interest.

ACKNOWLEDGMENTS

This research was funded by The Ministry of Education, Culture, Research, and Technology of Indonesia in 2024, grant number 047/SP2H/RT-MONO/LL4/2024. The authors gratefully acknowledge the Research Center for Radioisotope, Radiopharmaceutical, and Biodosimetry Technology and installation of Radioisotope and Radiopharmaceutical Technology (ITRR), Directorate of Facilities and Nucle-

ar Management, BRIN for supporting these research activities.

REFERENCES

Baldwin RM, Lin TH (1981) Chlorination as a side reaction in radioiodination with chloramine-T. J Radioanal Chem 65(1–2): 163–165. https://doi.org/10.1007/BF02516099

Bray F, Laversanne M, Sung H, Ferlay J, Siegel RL, Soerjomataram I, Jemal A (2024) Global cancer statistics 2022: GLOBOCAN estimates of incidence and mortality worldwide for 36 cancers in 185 countries. CA Cancer J Clin 74(3): 229–263. https://doi.org/10.3322/caac.21834

Choi MH, Rho JK, Kang JA, Shim HE, Nam YR, Yoon S, Kim HR, Choi DS, Park SH, Jang BS, Jeon J (2016) Efficient radiolabeling of rutin with ^{125}I and biodistribution study of radiolabeled rutin. J Radioanal Nucl Chem 308(2): 477–483. https://doi.org/10.1007/s10967-015-4415-8

Dagher Z, Borgie M, Magdalou J, Chahine R, Greige-Gerges H (2012) p-Hydroxybenzoate esters metabolism in MCF7 breast cancer cells. Food Chem Toxicol 50(11): 4109–4114. https://doi.org/10.1016/j.fct.2012.08.013

Daruwati I, Anggraini Y, Wangsaatmadja AH (2019) Labeling of piperine with iodine-131 as radiotracer in the development of cancer drugs from Indonesia's natural products. Indones J Pharm Sci Technol S1(3): 18–25. https://doi.org/10.24198/ijpst.v1i3.21031

Daruwati I, Gwiharto AK, Wongso H, Achmad TH, Syaifudin M, Muchtaridi M (2023) Method development, validation, and impurity measurement of β-estradiol from radiolabeled [^{131}I]β-estradiol using radio-high-performance liquid chromatography for radioligand of saturation binding assay. J Adv Pharm Technol Res 14(2): 105–112. https://doi.org/10.4103/japtr.japtr_624_22

Daruwati I, Halimah I, Mahendra I, Deasy FD, Hanafiah WSA (2017) *In vivo* interaction of propylthiouracil with sodium iodide (Na^{131}I) radiopharmaceutical in rats (*Rattus norvegicus*). J Sains Teknol Nuklir Indones 18(2): 85. https://doi.org/10.17146/jstni.2017.18.2.3439

Durante ACR, Sobral DV, Miranda ACC, de Almeida ÉV, Fuscaldi LL, de Barboza MRFF, Malavolta L (2019) Comparative study of two oxidizing agents, chloramine T and Iodo-Gen®, for the radiolabeling of β-CIT with iodine-131: Relevance for Parkinson's disease. Pharmaceuticals 12(1): 25. https://doi.org/10.3390/ph12010025

Iglesias ML, Schmidt A, Ghuzlan AA, Lacroix L, Vathaire F, Chevillard S, Schlumberger M (2017) Radiation exposure and thyroid cancer: A review. Arch Endocrinol Metab 61(2):180–187. https://doi.org/10.1590/2359-3997000000257

Kritsanawong S, Innajak S, Imoto M, Watanapokasin R (2016) Antiproliferative and apoptosis induction of α-mangostin in T47D breast cancer cells. Int J Oncol 48(5): 2155–2165. https://doi.org/10.3892/ijo.2016.3399

Lee CH, Ying TH, Chiou HL, Hsieh SC, Wen SH, Chou RH, Hsieh YH (2017) Alpha-mangostin induces apoptosis through activation of reactive oxygen species and ASK1/p38 signaling pathway in cervical cancer cells. Oncotarget 8(29): 47425–47439. https://doi.org/10.18632/oncotarget.17659

Li L, Brunner I, Han AR, Hamburger M, Kinghorn AD, Frye R, Butterweck V (2011) Pharmacokinetics of α-mangostin in rats after intravenous and oral application. Mol Nutr Food Res 55(suppl. 1): S67-S74. https://doi.org/10.1002/mnfr.201000511

Mahendra I, Daruwati I, Halimah I, Pajrin SR (2018) Pharmacokinetics interaction of nonsteroidal anti-inflammatory drugs with ^{99m}TC-MDP radiopharmaceuticals for bone imaging. Atom Indones 44(3): 173–177. https://doi.org/10.17146/aij.2018.741

Majdalawieh AF, Terro TM, Ahari SH, Abu-Yousef IA (2024) α-Mangostin: A xanthone derivative in mangosteen with potent anti-cancer properties. Biomolecules 14(11): 1382. https://doi.org/10.3390/biom14111382

Mardianingrum R, Endah SRN, Daruwati I, Muchtaridi M, Ruswanto R (2024) Synthesis and computational study of metal complex of α-mangostin as an anticancer candidate. J Pharm Pharmacogn Res 12(3): 423–438. https://doi.org/10.56499/jppres23.1827_12.3.423

Muftuler FZ, Unak P, Teksoz S, Acar C, Yolcular S, Yürekli Y (2008) ^{131}I labeling of tamoxifen and biodistribution studies in rats. Appl Radiat Isot 66(2): 178–187. https://doi.org/10.1016/j.apradiso.2007.08.005

Nurhidayah W, Widyasari EM, Daruwati I, Mahendra I, Subroto T, Khairul Ikram NK, Muchtaridi M (2023) Radiosynthesis, stability, lipophilicity, and cellular uptake evaluations of [^{131}I]Iodine-α-mangostin for breast cancer diagnosis and therapy. Int J Mol Sci 24(10): 8678. https://doi.org/10.3390/ijms24108678

Ruswanto R, Mardianingrum R, Nofianti T, Fizriani R, Siswandono S (2023) Computational study of bis-(1-(benzoyl)-3-methyl thiourea) platinum (II) complex derivatives as anticancer candidates. Adv Appl Bioinform Chem 16: 15–36. https://doi.org/10.2147/AABC.S392068

Silberstein EB, Alavi A, Balon HR, Clarke SE, Divgi C, Gelfand MJ, Goldsmith SJ, Jadvar H, Marcus CS, Martin WH, Parker JA, Royal HD, Sarkar SD, Stabin M, Waxman AD (2012) The SNMMI practice guideline for therapy of thyroid disease with ^{131}I 3.0. J Nucl Med 53(10): 1633–1651. https://doi.org/10.2967/jnumed.112.105148

Sriyani ME, Utami DA, Dwike MS, Widyasari EM, Marzuki M, Sugiharti RJ, Nuraeni W (2019) Synthesis of ^{131}I labeled quercetin through oxidation method using chloramine-T for cancer radiopharmaceuticals. Indones J Chem 19(4): 841-848. https://doi.org/10.22146/ijc.34512

Tishchenko VK, Petriev VM, Smoryzanova OA, Zavestovskaya IN (2017) A comparative analysis of pharmacokinetics properties of diagnostic bone-seeking radiopharmaceuticals on the basis of phosphonic acids and technetium-99m. J Phys: Conf Ser 784: 12045. https://doi.org/10.1088/1742-6596/784/1/012045

Vantangoli MM, Madnick SJ, Huse SM, Weston P, Boekelheide K (2015) MCF-7 human breast cancer cells form differentiated microtissues in scaffold-free hydrogels. PLoS One 10(8): e0135426. https://doi.org/10.1371/journal.pone.0135426

Won YS, Lee JH, Kwon SJ, Kim JY, Park KH, Lee MK, Seo KI (2014) α-Mangostin-induced apoptosis is mediated by estrogen receptor α in human breast cancer cells. Food Chem Toxicol 66: 158–165. https://doi.org/10.1016/j.fct.2014.01.040

Wongso H (2022) Natural product-based radiopharmaceuticals: Focus on curcumin and its analogs, flavonoids, and marine peptides. J Pharm Anal 12(3): 380–393. https://doi.org/10.1016/j.jpha.2021.07.006

Wongso H, Kurniawan A, Forentin AM, Susilo VY, Setiadi Y, Mahendra I, Febrian MB, Rosdianto AM, Setiawan I, Goenawan H, Susianti S, Supratman U, Widyasari EM, Wibawa THA, Sriyani ME, Halimah I, Lesmana R (2023) New hybrid radio-fluorescent probes [^{131}I]-BPF-01 and [^{131}I]-BPF-02 for visualisation of cancer cells: Synthesis and preliminary *in vitro* and *ex vivo* evaluations. Heliyon 9(10): e20710. https://doi.org/10.1016/j.heliyon.2023.e20710

Wongso H, Mahendra I, Arnafia W, Idar I, Yusuf M, Achmad A, Holik HA, Kurniawan A, Halimah I, Sriyani ME, Wibawa THA, Febrian MB, Setiadi Y, Widyasari EM, Daruwati I, Kusumaningrum CE, Subroto T (2022) Preclinical evaluation of chicken egg yolk antibody (IgY) anti-RBD spike SARS-CoV-

2—A candidate for passive immunization against COVID-19. Vaccines 10(1): 128. https://doi.org/10.3390/vaccines10010128

Yang S, Zhou F, Dong Y, Ren F (2021) α-Mangostin induces apoptosis in human osteosarcoma cells through ROS-mediated endoplasmic reticulum stress via the WNT pathway. Cell Transplantation, 30: 9636897211035080. https://doi.org/10.1177/09636897211035080

Zhang C, Xu C, Gao X, Yao Q (2022) Platinum-based drugs for cancer therapy and anti-tumor strategies. Theranostics 12(5): 2115–2132. https://doi.org/10.7150/thno.69424

Zhang P, Sadler PJ (2017) Advances in the design of organometallic anticancer complexes. J Organomet Chem 839: 5–14. https://doi.org/10.1016/j.jorganchem.2017.03.038

AUTHOR CONTRIBUTION:

Contribution	Mardianingrum R	Susanti S	Muchtaridi M	Ruswanto R	Suharyani I	Gozzali AM	Daruwati I	Fikri A	Rizaludin A	Forentin AM	Lestari W	Susilo VY	Ramadhani D	Tuasikal BJ
Concepts or ideas	x			x			x							
Design	x						x							
Definition of intellectual content		x	x				x			x			x	x
Literature search		x			x	x	x	x		x			x	
Experimental studies							x	x	x	x	x	x	x	x
Data acquisition	x						x	x	x	x	x	x	x	x
Data analysis		x							x		x		x	x
Statistical analysis	x		x				x	x	x				x	
Manuscript preparation	x		x				x	x	x	x	x		x	x
Manuscript editing	x				x	x	x	x		x				
Manuscript review	x	x	x	x	x	x	x	x	x	x	x	x	x	x

Citation Format: Mardianingrum R, Susanti S, Muchtaridi M, Ruswanto R, Suharyani I, Gozzali AM, Daruwati I, Fikri A, Rizaludin A, Forentin AM, Lestari W, Susilo VY, Ramadhani D, Tuasikal BJ (2025) Radioiodinated bis-(α-mangostin)-cobalt (II) ([^{131}I]I-AM-Co): Radiolabelling, *in vitro* and *in vivo* evaluation for breast cancer radiopharmaceutical. J Pharm Pharmacogn Res 13(4): 1110–1119. https://doi.org/10.56499/jppres24.2214_13.4.1110

Publisher's Note: All claims expressed in this article are solely those of the authors and do not necessarily represent those of their affiliated organizations, or those of the publisher, the editors and the reviewers. Any product that may be evaluated in this article, or claim that may be made by its manufacturer, is not guaranteed or endorsed by the publisher.

Open Access: This article is distributed under the terms of the Creative Commons Attribution 4.0 International License (http://creativecommons.org/ licenses/by/4.0/), which permits use, duplication, adaptation, distribution and reproduction in any medium or format, as long as you give appropriate credit to the original author(s) and the source, provide a link to the Creative Commons license and indicate if changes were made.